*J. Microbiol. Biotechnol.* (2010), **20**(12), 1647–1652
doi: 10.4014/jmb.1007.07061
First published online 29 September 2010

JOURNAL OF MICROBIOLOGY AND BIOTECHNOLOGY



# Purification and Characterization of a Ubiquitin-like System for Autophagosome Formation

**Bae, Ju Young[1] and Hyun Ho Park[1,2]***

[1]*Graduate school of Biochemistry, Yeungnam University, Gyeongsan 712-749, Korea*
[2]*School of Biotechnology, Yeungnam University, Gyeongsan 712-749, Korea*

Received: July 30, 2010 / Revised: August 27, 2010 / Accepted: August 28, 2010

**Autophagy refers to the bulk degradation of cellular proteins and organelles through an autophagosome and plays a pivotal role in the development, cellular differentiation, aging, and elimination of aberrant structures. A failure of autophagy has been implicated in a growing list of mammalian disease states, including cancer and cardiomyopathy. Two ubiquitin-like systems are highly involved in autophagy, especially in the formation of autophagosomes. Here, we purified and characterized Atg7 (an E1-like enzyme), and Atg3 and Atg10 (E2-like enzymes) in order to gain an insight into the role played by ubiquitin-like systems in the formation of autophagosomes. Interestingly, we observed that Atg7 forms a homodimer to construct an active conformation, unlike other E1-like enzymes. Although Atg3 was detected as a monomer under physiological conditions, Atg10 existed in an oligomeric form, indicating that the mechanism by which Atg10 functions may differ from that of Atg3.**

**Keywords:** Autophagy, Atg3, Atg7, Atg10, autophagosome, ubiquitin, E1-like enzyme, E2-like enzyme

To ensure the proper homeostasis of cellular organelles and cellular proteins, especially under extreme environmental conditions such as starvation and in response to various developmental clues or pathological insults, cells must be able to control their biosynthesis and degradation. This balance is primarily accomplished by a unique membrane trafficking process known as autophagy, which refers to the bulk degradation of cellular proteins and organelles through an autophagosome-mediated lysosomal pathway [3, 6]. Although autophagy was observed in the early 1960s as a simple transport pathway from the cytoplasm to lysosomes/vacuoles that enables the turnover of cellular components, the importance of this process has only recently been recognized as the understanding of autophagy at the molecular level has increased [20]. It is now widely accepted that autophagy actively participates in many cellular processes including development, cellular differentiation, aging, the elimination of aberrant structures, and non-apoptotic programmed cell death [4, 10, 11, 15, 19]. Moreover, the failure of autophagy has been implicated in a growing list of mammalian disease states, including cancer, cardiomyopathy associated with Danon's disease, and neurodegenerative disorders [10, 15]. Therefore, an understanding of the molecular mechanisms involved in autophagic signaling and the identification of chemicals or drugs that can control autophagy should facilitate a greater degree of control over the aforementioned diseases. Despite the functional importance of autophagy in many critical cellular processes, our current understanding of autophagy at the structural level is insufficient, especially at the step of autophagosome formation.

In yeast, autophagy is maintained at a low basal level under nutrient-rich conditions. Upon nutrient starvation, autophagy is up-regulated, which results in the production of amino acids and other macromolecules necessary for survival [2]. This process can be divided into the following 4 distinct steps: (1) induction by Tor-mediated signal transduction events under starvation conditions; (2) formation of double lipid layer membrane vesicles, known as autophagosomes, that sequester cytosolic proteins and organelles nonselectively; (3) docking and fusion of autophagosomes with their target vacuole/lysosomes; and (4) breakdown of autophagic bodies within the vacuoles in order to allow for the recycling of the hydrolyzed cargo [1, 8, 9, 17, 18]. Screening of yeast for autophagy-defective mutants led to the identification of at least 16 genes required for autophagosome formation [8]. Among these, two ubiquitin (Ub)-like systems were found to be tightly involved in autophagy, especially in the formation of autophagosomes [7, 12, 13]. These systems are the Atg12 conjugation system and the Atg8 lipidation system [7]. Atg12 is a hydrophilic protein, composed of 186 amino

*Corresponding author
Phone: +82-53-810-3033; Fax: +82-53-810-4769;
E-mail: hyunho@ynu.ac.kr

acids, that has no apparent homology to ubiquitin. However, Atg12 forms a conjugate with the target molecule, Atg5, through the ubiquitin-like system. As in the ubiquitin system, the carboxy-terminal glycine residue of Atg12 is activated by the E1-like enzyme, Atg7. Subsequently, Atg12 is transferred to an E2 enzyme, Atg10, which results in the formation of a thioester bond and conjugation to Atg5 [14, 16]. The Atg12–Atg5 complex further recruits a small coiled-coil protein, Atg16, which results in the formation of a ~350 kDa protein complex in yeast and a ~800 kDa complex in mammalian cells.

The Atg8 lipidation system is mediated by the ubiquitin-like 117-residue small protein, Atg8. Atg8 is processed at its end *via* the cleavage of a single amino acid, which leaves the glycine residue at the carboxyl terminus [5, 21]. This exposed glycine is necessary for conjugation with Atg7 (E1) and then with Atg3 (E2), which occurs through a thioester bond in both cases. Finally, Atg8 is transferred to phosphatidylethanolamine (PE). This transient membrane attachment of Atg8 is necessary for autophagosome formation. Conjugated Atg8 is deconjugated by the deconjugation enzyme, Atg4 [5, 21]. Although it remains unclear how these two conjugation systems and their complex product are involved in the formation of autophagosomes, it is known that they are essential for this process.

In order to facilitate a better understanding of the molecular basis of autophagosome formation, we purified the proteins involved in the Ub-like system mediating autophagosome formation. Further biochemical characterization revealed that the E1-like protein, Atg7, is homodimerized in solution, unlike other E1-like proteins. Based on the domain organization and sequence alignment of Atg7 with other E1-like enzymes, such as ubiquitine-E1, SUMO-E1, and NEDD8-E1, the homodimerization may be the critical mechanism involved in the induction of the enzymatic activity of Atg7. It was noted that Atg3, the E2-like protein involved in the Atg8 lipidation system, exists as a stable monomer under physiological conditions. Additionally, we observed that Atg10, another E2-like protein involved in the Atg12 conjugation system, can easily alter oligomeric states based on the concentration of salt.

## Materials and Methods

### Sequence Alignment

The amino acid sequence of each E1-like enzyme was analyzed using ClustalW (http://www.ebi.ac.kr/Tools/clustalw2/index.html) and BLAST-n (http://blast.ncbi.nlm.nih.gov/Blast.cgi).

### Generation of Atg7 Bacmid

To produce the Atg7 protein using the baculovirus expression system, an Atg7 bacmid was constructed. To accomplish this, the full-length Atg7 was subcloned into the pFastBac HT A vector using the *Bam*HI and *Xho*I sites. The Atg7-containing pFastBac vector was then transformed into DH10Bac cells using the same method employed to produce normal constructs. The transformation SOC solution diluted by 1/100 was then plated on LB agar plates containing kanamycin, gentamicin, tetracycline, IPTG, and blue-gal (tetracycline dissolved in ethanol and Blue-gal dissolved in DMSO). Next, the samples were incubated for 48 h at 37°C, after which white colonies were streaked onto new plates. After 48 h of incubation at 37°C, an isolated colony was selected and cultured in 5 ml of LB media at 37°C for 9 h. The cells were then transferred to 500 ml of LB media for maxi-prep, which was conducted using a Promega maxi-prep kit. The purified bacmid was then evaluated by PCR using M13 forward/reverse primers.

### Protein Expression and Purification in Insect Cells

Hi5 cells grown in 2-l aerated spinner flasks in SF-9 medium were infected with Atg7 viruses at a density of $2\times10^6$ cells/ml and harvested 72 h post-infection. The cells were then resuspended in a 50 ml lysis buffer (20 mM Tris at pH 7.9, 500 mM NaCl, and 5 mM imidazole) supplemented with a complete protease inhibitor mixture (Roche Diagnostics, USA), after which they were disrupted by sonication. The cell debris was then removed by centrifugation (95,000 ×*g*, 1 h, 4°C) and the supernatant applied to a gravity-flow column (Bio-Rad) packed with Ni-NTA affinity resin (Qiagen, USA). The unbound proteins were then removed from the column using a wash buffer (20 mM Tris at pH 7.9, 500 mM NaCl, 60 mM imidazole, and 10% glycerol), and the C-terminal His-tagged Atg7 was subsequently eluted from the column using an elution buffer (20 mM sodium phosphate and 300 mM imidazole). The elution fractions were further purified by anion-exchange chromatography on Q-Separose (Pharmacia Biotech, USA) using a 20 mM phosphate buffer containing 5 mM DTT as a starting buffer with a gradient of NaCl (50~1,000 mM). Fractions that contained Atg7 were collected and concentrated using Centriprep (cut off 30). The concentrated protein was then applied to a Superdex 200 gel filtration column 10/30 (Pharmacia Biotech, USA) that had been preequilibrated with a solution of 20 mM Tris at pH 8.0, 100 mM NaCl, and 2 mM DTT. The peak fractions were then confirmed by SDS–PAGE.

### Protein Expression and Purification in *E. coli*

Atg3 (1-314) in the pET28a vector, which adds an eight-residue N-terminal hexahistidine tag (LEHHHHHH), was generously donated by Dr. Jiang at MSKCC. The plasmid was transformed into BL21 (DE3) *E. coli* competent cells, after which expression was induced by treatment with 0.5 mM IPTG for 20 h at 20°C. The bacteria were then collected, resuspended, and lysed by sonication in a 50 ml lysis buffer (20 mM Tris buffer at pH 7.9, 500 mM NaCl, and 5 mM imidazole) supplied with a protease cocktail (Roche, USA). The bacterial lysate was then centrifuged at 16,000 rpm for 1 h at 4°C, after which the supernatant fraction was applied to a gravity-flow column (Bio-Rad, USA) packed with Ni-NTA affinity resin (Qiagen, USA). Next, the unbound bacterial proteins were removed from the column using a washing buffer (20 mM Tris buffer at pH 7.9, 500 mM NaCl, 60 mM imidazole, and 10% glycerol). The N-terminal His6-tagged Atg3 was subsequently eluted from the column using an elution buffer (20 mM Tris buffer at pH 8.0, 500 mM NaCl, and 250 mM imidazole). The protein purity was

further improved by passing the sample through a Superdex 200 gel filtration column 10/30 (GE Healthcare, USA) in a solution of 20 mM Tris buffer at pH 8.0, 50 mM NaCl and 2 mM DTT.

The construct used to express the full-length Atg10 was produced using the polymerase chain reaction (PCR) and plasmid vector pET28a (Novagen, USA), which was employed to add a hexahistidine tag to the N-terminus of Atg10 for affinity purification. The expression and purification methods used for Atg10 were the same as those used for Atg3, except for the fact that two buffers were used for the gel filtration chromatography. Buffer 1 contained a 20 mM Tris buffer at pH 8.0, 50 mM NaCl, and 1 mM DTT, and buffer 2 contained a 20 mM Tris buffer at pH 8.0, 150 mM NaCl, and 1 mM DTT.

**Analytical Size-Exclusion Chromatography**

A 1-ml sample containing 10 mg of purified proteins was applied to a Superdex 200 gel filtration column 10/30 (GE Healthcare) that had been equilibrated with a 20 mM Tris buffer at pH 8.0, 50~150 mM NaCl, and 2 mM DTT. The UV profile during chromatography was monitored at 280 nm. For calibration of the column with known molecular masses, the following compounds were used: thyroglobins (670 kDa), bovine gamma-globulin (158 kDa), chicken ovalbumin (44 kDa), equine myoglobin (17 kDa), and vitamin $B_{12}$ (1.35 kDa).

**Native-PAGE**

The oligomerization state was assayed by native-PAGE conducted on a PhastSystem (GE Healthcare) with pre-made 8–25% acrylamide

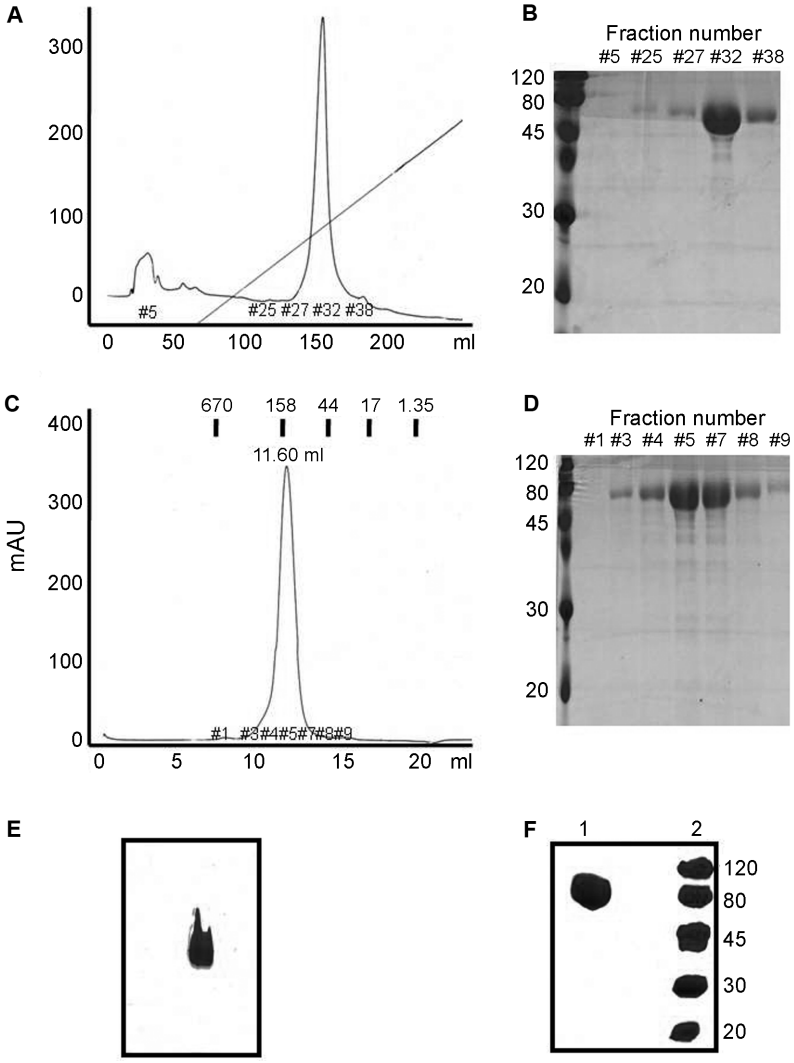


**Fig. 1.** Purification and characterization of Atg7 using insect cells as hosts.

**A**. Ion-exchange profile showing the eluted position of Atg7. The line shows a NaCl gradient from 50 mM to 1 M. The number of fractions subjected to SDS–PAGE is shown below the peak. **B**. SDS–PAGE of the ion-exchange fractions showing the identity and purity of Atg7. **C**. Gel filtration profile showing the eluted position of Atg7. The number of fractions subjected to SDS–PAGE is shown below the peak. Calibration standards are shown above the peak. **D**. SDS–PAGE of the gel filtration fractions showing the identity and purity of Atg7. **E**. Native-PAGE analysis of the homogeneity of Atg7. The prepared Atg7 was loaded onto an 8~25% premade native gel and stained with Coomassie blue. **F**. SDS–PAGE showing the final sample of Atg7. Lane 1: purified Atg7; Lane 2: Size marker. The purified sample was loaded onto a 15% SDS–PAGE gel and stained with Coomassie blue.

gradient gels (GE Healthcare). Coomassie Brilliant Blue was used for staining.

## Results and Discussion

### Purification and Characterization of the Atg7 (E1-like) Enzyme

We first attempted to express Atg7 in *E. coli*, but were unsuccessful; therefore, we used the baculovirus-mediated insect cell expression system. Hi5 cells grown in a SF-9 medium were infected with viruses containing Atg7 and harvested. The cells were then disrupted by sonication and the cell debris was removed by centrifugation. The supernatant was then applied to Ni-NTA affinity resin for affinity chromatography. The C-terminal His-tagged Atg7 was eluted from the affinity column by 250 mM imidazole and further purified by anion-exchange chromatography on Q-Separose. The C-terminal His-tagged Atg7 was eluted using around 200 mM NaCl (Fig. 1A), and the Atg7 peak fractions from the anion-exchange chromatography were subjected to SDS–PAGE (Fig. 1B). Fractions that contained Atg7 were collected, concentrated, and then applied to a Superdex 200 gel filtration column that had been preequilibrated with 20 mM Tris at pH 8.0, 100 mM NaCl, and 2 mM DTT. Atg7 was eluted at 11.60 ml, which corresponded to a molecular mass of 150~180 kDa (Fig. 1C). The peak fractions were then confirmed by SDS–PAGE (Fig. 1D). The purified recombinant Atg7 migrated as a single band of approximately 80 kDa during SDS–PAGE. However, gel-filtration analysis estimated the protein to have a mass of approximately 160 kDa, suggesting that Atg7 exists as a homodimer, which distinguishes it from other E1-like enzymes. Native-PAGE showed a clean single band on the gel, which indicated that the Atg7 homodimers tightly interacted with one another and existed in solution with high homogeneity (Fig. 1E and 1F).

Although the weak sequence similarity to E1-like enzymes makes it difficult to predict the domain boundary and structure, the functional domain composition calculated, using BLAST-n and ClustalW, indicates that these enzymes consist of an adenylation domain, a catalytic domain, and a ubiquitin-like domain at the C-terminus (Fig. 2). NEDD8-E1 and SUMO-E1 are encoded on two separate polypeptide chains, ABBPB1 and UBA3 for NEDD8-E1, and Sae1 and Sae2 for SUMO-E1. Ub-E1 is encoded by a single open reading frame with sequences that are similar to ABBPB1 and Sae1 in its N-terminal portion, and to UBA3 and Sae2 in its C-terminal part. The catalytic cysteine domain is discontinuous and interspersed into the adenylation domain. To form a fully functional catalytic domain, the two separate catalytic cysteine domains must be combined. Although NEDD8-E1 (or Sumo-E1) and Ub-E1 use different mechanisms, both enzymes possess

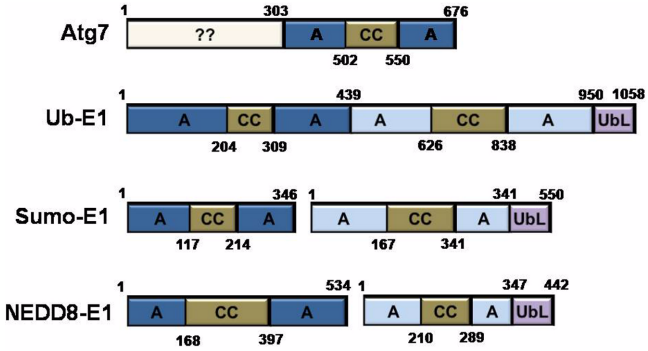


**Fig. 2.** Domain organization mapped to a linear sequence for the E1-like enzymes.
The domain boundary was calculated using Clustal W (http://www.ebi.ac.kr/Tools/clustalw2/index.html) and BLAST-n (http://blast.ncbi.nlm.nih.gov/Blast.cgi). The adenylation half-domains are shown in dark and light blue, the cysteine catalytic domain is shown in gold, and the UbL domain is shown in pink. A, adenylation domain; CC, cysteine catalytic domain; UbL, ubiquitin-like domain.

two catalytic cysteine domains that consist of two different polypeptide chains, or two cysteine domains, on a single polypeptide chain (Fig. 2). Based on a domain boundary search and sequence alignment using BLAST-n and

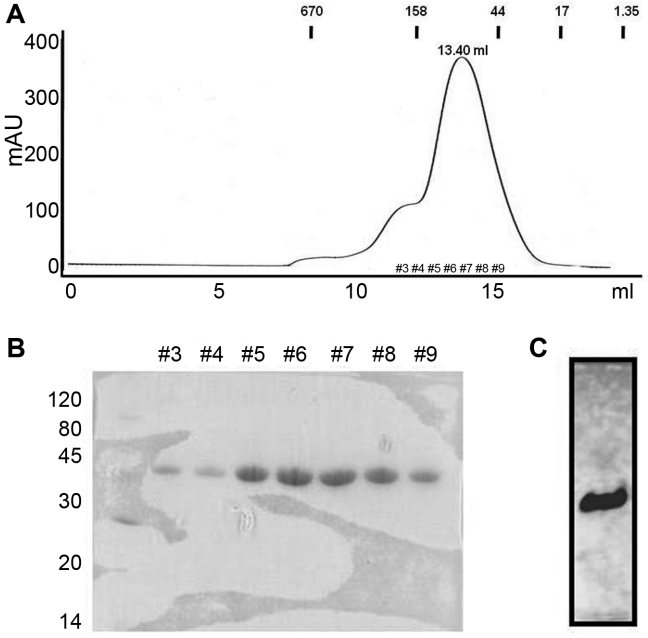


**Fig. 3.** Purification and characterization of Atg3 using *E. coli* as the host.
**A**. Gel filtration profile showing the eluted position of Atg3. The number of fractions loaded onto the SDS–PAGE is shown below the peak. Calibration standards are shown above the peak. **B**. SDS–PAGE of the gel filtration fractions showing the identity and purity of Atg3. **C**. Native-PAGE analysis of the homogeneity of Atg3. Prepared samples of Atg3 were loaded onto an 8~25% premade native gel and stained with Coomassie blue.

ClustalW, we found that Atg7 has two adenylation domains (303–502 and 550–676), one catalytic domain (502–550), and an unknown domain at the N-terminal (1–303). Atg7 does not exist as a heterodimer like NEDD8-E1(or Sumo-E1) and does not contain two catalytic cysteine domains in the single polypeptide chain like Ub-E1. Based on the fact that Atg7 exists as a homodimer in solution, the working mechanism of Atg7 may be to form a homodimer for the formation of two cysteine catalytic domains. This may represent a novel catalytic mechanism among E1-like enzymes.

**Purification and Characterization of the Atg3 (E2-like) Enzyme**

The Atg3 construct (1–314) created using the pET28a vector was transformed into BL21 (DE3) *E. coli* competent cells. Expression was then induced by treating the bacteria with 0.5 mM IPTG for 20 h at 20°C. The bacteria were then collected, resuspended, and lysed by sonication. Next, the bacterial lysate was centrifuged and the supernatant fraction was applied to a gravity-flow column (Bio-Rad, USA) packed with Ni-NTA affinity resin. The unbound bacterial proteins were then removed from the column using a washing buffer, after which the N-terminal His6-tagged Atg3 was eluted from the column using an elution buffer containing a 20 mM Tris buffer at pH 8.0, 500 mM NaCl, and 250 mM imidazole. Next, the eluted protein was applied onto a Superdex 200 gel filtration column 10/30 (GE Healthcare) and then eluted with a 20 mM Tris buffer at a pH of 8.0, 50 mM NaCl, and 2 mM DTT. The peak containing Atg3 was eluted at 13.40 ml (Fig. 3A). The peak fractions were subsequently loaded onto a SDS-PAGE gel to check their identity and purity (Fig. 3B). The results revealed that a 99% pure, homogeneous Atg3 protein was prepared by the two chromatography steps (Fig. 3C).

The calculated molecular mass of Atg3 with hexahistidine is 39,864.3 Da. Based on the peak position, the possible molecular mass of Atg3 in solution is approximately 40~60 kDa, which indicates that Atg3 may exist as a monomer. Although Atg3 has little sequence homology with other E2-like enzymes, its working mechanism is likely similar to that of a canonical E2-like enzyme.

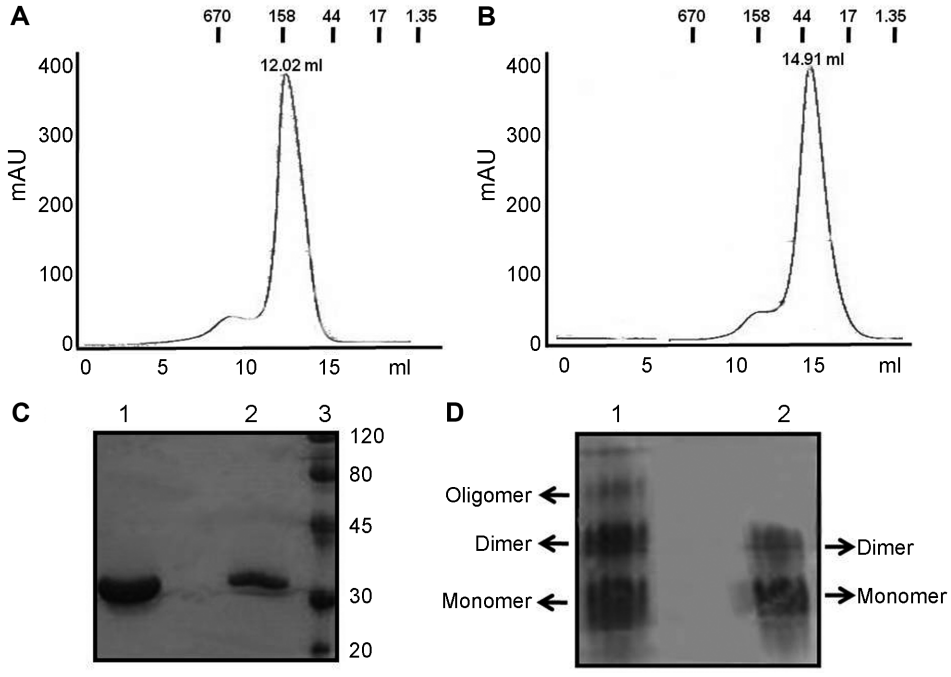


**Fig. 4.** Purification and characterization of Atg10 using *E. coli* as the host.

**A**. Gel filtration profile showing the eluted position of Atg10 in a buffer composed of 20 mM Tris-HCl at pH 8.0, 50 mM NaCl, and 1 mM DTT. Calibration standards are shown above the peak. **B**. Gel filtration profile showing the eluted position of Atg10 in a buffer containing 20 mM Tris-HCl at pH 8.0, 150 mM NaCl, and 1 mM DTT. Calibration standards are shown above the peak. The eluted position of the peak is shown. **C**. SDS–PAGE of Atg10 purified under two different conditions showing the identity and purity of Atg3. Lane 1, Purified Atg10 in a buffer composed of 20 mM Tris-HCl at pH 8.0, 50 mM NaCl, and 1 mM DTT; Lane 2, Purified Atg10 in a buffer composed of 20 mM Tris-HCl at pH 8.0, 150 mM NaCl, and 1 mM DTT; Lane 3, Protein marker. **D**. Native-PAGE analysis of the homogeneity of Atg10 showing the existence of the oligomeric form of Atg10. A prepared sample of Atg10 was loaded onto an 8~25% premade native gel and stained with Coomassie blue. Lane 1, Purified Atg10 in a buffer composed of 20 mM Tris-HCl at pH 8.0, 50 mM NaCl, and 1 mM DTT. The dimer, tetramer, and further oligomeric forms are shown on the native gel; Lane 2, Purified Atg10 in buffer composed of 20 mM Tris-HCl, pH 8.0, 150 mM NaCl, and 1 mM DTT. Only the dimer form was detected.

### Purification and Characterization of the Atg10 (E2-like) Enzyme

The construct used for the expression of full-length Atg10 was made using a polymerase chain reaction and the pET28a plasmid vector, which was employed to add a hexahistidine tag at the N-terminus of Atg10 for affinity purification, after which the resulting plasmid was transformed into BL21 (DE3) *E. coli* competent cells. The expression was induced by treating the bacteria with 0.5 mM isopropyl β-D-thiogalactopyranoside (IPTG) overnight at 20°C. The bacteria were then collected, resuspended, and lysed by sonication, after which the bacterial debris were removed by centrifugation and the supernatant fraction was applied to a Hitrap 5-ml column. The unbound bacterial proteins were removed from the column using a washing buffer, and the resin-bound Atg10 was then eluted from the column using an elution buffer containing 50 mM phosphate buffer at pH 8.0, 500 mM NaCl, 300 mM imidazole, and 1 mM TCEP (Tris-2-carboxyethyl phosphine). The protein purity was further improved by applying the samples to a Superdex 200 gel filtration column that had been preequilibrated with either buffer 1 or buffer 2. Interestingly, Atg10 was eluted at around 12.02 ml when buffer 1 was used (Fig. 4A), whereas it was eluted at around 14.91 ml when buffer 2 was used (Fig. 4B). These findings indicate that Atg10 is prone to changes in its oligomeric state, and that these changes are sensitive to the concentration of NaCl. The final purified product was evaluated by SDS–PAGE and native-PAGE (Fig. 4C and 4D). Although SDS–PAGE indicated that the protein was extremely pure (approximately 99% purity), analysis on native gel revealed that Atg10 was heterogeneous and formed dimers, tetramers, and even higher order oligomers. Additionally, Atg10 was found to be in a much higher oligomeric form in buffer A, which contained less NaCl.

Protein components involved in the ubiquitin-like system for autophagy were purified in this study. We found that Atg7 dimerization was critical for the activity of Atg7. Unlike other E1-like enzymes, Atg7 may be homodimerized, so as to produce two cysteine catalytic domains. Purified Atg3 and Atg10 perform their activity in different ways. Atg3 displays the ability to work as a monomer under physiological conditions, whereas the oligomeric state of Atg10 changes easily, based on the concentration of salt. The importance of this latter oligomeric form should be addressed.

## Acknowledgment

This study was supported by way of a grant (A084512) from the Korea Healthcare Technology R&D Project, part of the Ministry of Health, Welfare and Family Affairs, in the Republic of Korea.

## References

1. Abeliovich, H., W. A. Dunn Jr., J. Kim, and D. J. Klionsky. 2000. Dissection of autophagosome biogenesis into distinct nucleation and expansion steps. *J. Cell Biol.* **151:** 1025–1034.
2. Abeliovich, H. and D. J. Klionsky. 2001. Autophagy in yeast: Mechanistic insights and physiological function. *Microbiol. Mol. Biol. Rev.* **65:** 463–479.
3. Davenport, E. L., L. I. Aronson, and F. E. Davies. 2009. Starving to succeed. *Autophagy* **5:** 1052–1054.
4. Eisenberg-Lerner, A., S. Bialik, H. U. Simon, and A. Kimchi. 2009. Life and death partners: Apoptosis, autophagy and the cross-talk between them. *Cell Death Differ.* **16:** 966–975.
5. Geng, J. and D. J. Klionsky. 2008. The Atg8 and Atg12 ubiquitin-like conjugation systems in macroautophagy. 'Protein modifications: Beyond the usual suspects' review series. *EMBO Rep.* **9:** 859–864.
6. He, C. and D. J. Klionsky. 2009. Regulation mechanisms and signaling pathways of autophagy. *Annu. Rev. Genet.* **43:** 67–93.
7. Ichimura, Y., T. Kirisako, T. Takao, Y. Satomi, Y. Shimonishi, N. Ishihara, *et al*. 2000. A ubiquitin-like system mediates protein lipidation. *Nature* **408:** 488–492.
8. Kim, J. and D. J. Klionsky. 2000. Autophagy, cytoplasm-to-vacuole targeting pathway, and pexophagy in yeast and mammalian cells. *Annu. Rev. Biochem*. **69:** 303–342.
9. Klionsky, D. J. and S. D. Emr. 2000. Autophagy as a regulated pathway of cellular degradation. *Science* **290:** 1717–1721.
10. Lee, J. A. 2009. Autophagy in neurodegeneration: Two sides of the same coin. *BMB Rep.* **42:** 324–330.
11. Meijer, A. J. and P. Codogno. 2009. Autophagy: Regulation and role in disease. *Crit. Rev. Clin. Lab. Sci.* **46:** 210–240.
12. Mizushima, N., T. Noda, T. Yoshimori, Y. Tanaka, T. Ishii, M. D. George, D. J. Klionsky, M. Ohsumi, and Y. Ohsumi. 1998. A protein conjugation system essential for autophagy. *Nature* **395:** 395–398.
13. Mizushima, N., H. Sugita, T. Yoshimori, and Y. Ohsumi. 1998. A new protein conjugation system in human. The counterpart of the yeast Apg12p conjugation system essential for autophagy. *J. Biol. Chem.* **273:** 33889–33892.
14. Mizushima, N., T. Yoshimori, and Y. Ohsumi. 2003. Role of the Apg12 conjugation system in mammalian autophagy. *Int. J. Biochem. Cell Biol.* **35:** 553–561.
15. Morselli, E., L. Galluzzi, O. Kepp, J. M. Vicencio, A. Criollo, M. C. Maiuri, and G. Kroemer. 2009. Anti- and pro-tumor functions of autophagy. *Biochim. Biophys. Acta* **1793:** 1524–1532.
16. Ohsumi, Y. and N. Mizushima. 2004. Two ubiquitin-like conjugation systems essential for autophagy. *Semin. Cell Dev. Biol.* **15:** 231–236.
17. Reggiori, F. and D. J. Klionsky. 2002. Autophagy in the eukaryotic cell. *Eukaryot. Cell* **1:** 11–21.
18. Stromhaug, P. E. and D. J. Klionsky. 2001. Approaching the molecular mechanism of autophagy. *Traffic* **2:** 524–531.
19. Van Limbergen, J., C. Stevens, E. R. Nimmo, D. C. Wilson, and J. Satsangi. 2009. Autophagy: From basic science to clinical application. *Mucosal Immunol.* **2:** 315–330.
20. Wang, C. W. and D. J. Klionsky. 2003. The molecular mechanism of autophagy. *Mol. Med.* **9:** 65–76.
21. Xie, Z., U. Nair, and D. J. Klionsky. 2008. Atg8 controls phagophore expansion during autophagosome formation. *Mol. Biol. Cell* **19:** 3290–3298.